The EMBO Journal (2008) 27, 1791–1803 | © 2008 European Molecular Biology Organization | All Rights Reserved 0261-4189/08
www.embojournal.org

THE EMBO JOURNAL

Sequential Cyk-4 binding to ECT2 and FIP3 regulates cleavage furrow ingression and abscission during cytokinesis

Glenn C Simon[1], Eric Schonteich[1], Christine C Wu[2], Alisa Piekny[3], Damian Ekiert[3,5], Xinzi Yu[4], Gwyn W Gould[4], Michael Glotzer[3] and Rytis Prekeris[1,*]

[1]Department of Cellular and Developmental Biology, School of Medicine, University of Colorado Health Sciences Center, Aurora, CO, USA, [2]Department of Pharmacology, School of Medicine, University of Colorado Health Sciences Center, Aurora, CO, USA, [3]Department of Molecular Genetics and Cell Biology, University of Chicago, Chicago, IL, USA and [4]Henry Wellcome Laboratory of Cell Biology, Division of Biochemistry and Molecular Biology, Institute of Biomedical and Life Sciences, University of Glasgow, Glasgow, UK

Cytokinesis is a highly regulated and dynamic event that involves the reorganization of the cytoskeleton and membrane compartments. Recently, FIP3 has been implicated in targeting of recycling endosomes to the mid-body of dividing cells and is found required for abscission. Here, we demonstrate that the centralspindlin component Cyk-4 is a FIP3-binding protein. Furthermore, we show that FIP3 binds to Cyk-4 at late telophase and that centralspindlin may be required for FIP3 recruitment to the mid-body. We have mapped the FIP3-binding region on Cyk-4 and show that it overlaps with the ECT2-binding domain. Finally, we demonstrate that FIP3 and ECT2 form mutually exclusive complexes with Cyk-4 and that dissociation of ECT2 from the mid-body at late telophase may be required for the recruitment of FIP3 and recycling endosomes to the cleavage furrow. Thus, we propose that centralspindlin complex not only regulates acto-myosin ring contraction but also endocytic vesicle transport to the cleavage furrow and it does so through sequential interactions with ECT2 and FIP3.

The EMBO Journal (2008) **27,** 1791–1803. doi:10.1038/emboj.2008.112; Published online 29 May 2008
Subject Categories: membranes & transport; cell cycle
Keywords: Cyk-4; cytokinesis; endosomes; FIP3; Rab11

Introduction

Cytokinesis is a highly regulated and dynamic event that involves many different cellular pathways. At least two distinct processes have an important function during cytokinesis. First, the cellular cytoskeleton must be extensively remodelled for the initiation, formation and ingression of the cleavage furrow. Second, the membrane must be delivered to the cleavage furrow to allow for furrow ingression and subsequently, at the terminal step of cytokinesis, abscission. Thus, tightly controlled temporal and spatial coordination of cytoskeleton remodelling and membrane trafficking are required for successful completion of cell division (for review, see Prekeris and Gould, 2008.

The centralspindlin complex is a key complex that regulates the formation of the central spindle and the acto-myosin contractile ring (Yuce *et al*, 2005; Zhao and Fang, 2005; Kamijo *et al*, 2006; Nishimura and Yonemura, 2006). Centralspindlin is comprised of Cyk-4/MgcRacGAP (hereafter Cyk-4), and MKLP1/ZEN-4/Pavarotti (hereafter MKLP1) (Mishima *et al*, 2002; Yuce *et al*, 2005). Cyk-4 is a GTPase-activating protein (GAP) for Rho family GTPases (Toure *et al*, 1998; Jantsch-Plunger *et al*, 2000), which forms a complex with MKLP1. Recent evidence has revealed that in addition to mid-zone microtubule bundling, centralspindlin recruits RhoGEF ECT2 (Yuce *et al*, 2005; Zhao and Fang, 2005). It has been suggested that upon its recruitment to the mid-zone, ECT2 activates RhoA and as a result regulates contractile ring function (Yuce *et al*, 2005; Zhao and Fang, 2005; Chalamalasetty *et al*, 2006; Kamijo *et al*, 2006).

Membrane delivery during cytokinesis is also critical for cell division (for review, see Baluska *et al*, 2006). Membrane delivery to the site of division is necessary in many different organisms including mammalian cells, *Xenopus laevis*, *Caenorhabditis elegans*, as well as in *Drosophila melanogaster* syncitial embryos (Skop *et al*, 2001; Shuster and Burgess, 2002; Riggs *et al*, 2003; Schweitzer *et al*, 2005; Boucrot and Kirchhausen, 2007). However, the source of the membrane delivered to the furrow remains to be fully understood. Several internal stores of membrane have been implicated for this process, including the trans-Golgi network (TGN) and endosomes. TGN-derived, VAMP8-containing secretory vesicles have been shown to be required for cell division (Low *et al*, 2003). It was proposed that these vesicles dock at the mid-body via interaction with centriolin and the exocyst complexes and mediate the abscission step of cytokinesis (Fielding *et al*, 2005; Gromley *et al*, 2005). In addition to TGN, recycling endosomes are also important for cytokinesis (Prekeris, 2003; Fielding *et al*, 2005; Wilson *et al*, 2005). Interestingly, the exocyst complex has also been implicated in targeting endocytic organelles to the cleavage furrow, presumably via interactions with either Arf6 or Rab11 GTPases (Fielding *et al*, 2005; Gromley *et al*, 2005; Chen *et al*, 2006).

Rab11-FIP3/Eferin/arfophillin (hereafter FIP3) belongs to a class II Rab11 family interacting proteins (Hales *et al*, 2001; Prekeris *et al*, 2001; Meyers and Prekeris, 2002; Hickson *et al*, 2003; Horgan *et al*, 2004) that has been previously shown to be required for the abscission step of cytokinesis (Wilson

*Corresponding author. Department of Cellular and Developmental Biology, School of Medicine, University of Colorado Health Sciences Center, 12801 E 17th Avenue, Aurora, CO 80045, USA.
Tel.: +1 303 724 3411; Fax: +1 303 724 3420;
E-mail: Rytis.Prekeris@uchsc.edu
[5]Present Address: The Scripps Research Institute, 10550 N Torrey Pines Road, La Jolla, CA 92037, USA

Received: 11 December 2007; accepted: 14 May 2008; published online: 29 May 2008

et al, 2005). Consistent with this, the FIP3 homologue in *D. melanogaster*, known as nuclear fallout (Nuf), was also shown to regulate cellularization (Rothwell *et al*, 1998; Riggs *et al*, 2003). FIP3 was originally identified as a protein that interacts with Rab11 and Arf6 GTPases (Prekeris *et al*, 2001; Riggs *et al*, 2003) and both Rab11 and Ar6 regulate recycling endosome targeting to the cleavage furrow during cytokinesis (Hickson *et al*, 2003). It has been suggested that FIP3 is recruited to recycling endosomes by binding to Rab11 (Hickson *et al*, 2003; Wilson *et al*, 2005). FIP3-containing endosomes associate with centrosomes until late telophase, when they rapidly translocate to the cleavage furrow (Fielding *et al*, 2005; Wilson *et al*, 2005). FIP3 is required for the successful completion of cytokinesis, as knock down of FIP3 by siRNA or overexpression of FIP3 dominant-negative mutants inhibit abscission (Wilson *et al*, 2005).

The molecular mechanisms regulating the targeting of FIP3-containing endosomes to the cleavage furrow during abscission remain to be fully understood. Here, using proteomic analysis we identify Cyk-4 as a FIP3-binding protein. We show that FIP3 binds to Cyk-4 at late telophase and that the centralspindlin complex is required for FIP3 recruitment to the mid-body. We also map the FIP3-binding region on Cyk-4 and show that it overlaps with the ECT2-binding domain. Finally, we demonstrate that FIP3 and ECT2 form mutually exclusive complexes with Cyk-4 and that removal of ECT2 from the centralspindlin complex at late telophase is required for the recruitment of FIP3-containing endosomes to the cleavage furrow. Thus, we propose that the centralspindlin complex regulates the recruitment of endocytic vesicles to the cleavage furrow at late telophase by sequential interactions with ECT2 and FIP3 proteins.

Results

Cyk-4/MgcRacGAP is a FIP3-binding protein

FIP3 has an important function in the regulation of endocytic vesicle targeting to the cleavage furrow during cytokinesis, and mediates the abscission of daughter cells (Hickson *et al*, 2003; Horgan *et al*, 2004; Fielding *et al*, 2005; Wilson *et al*, 2005). However, the mechanisms by which FIP3 performs these roles remain to be fully understood. Recently published structures of FIP3/Rab11 and FIP2/Rab11 complexes demonstrate that Rab11 binds to the extreme C terminus of the FIPs (Eathiraj *et al*, 2006; Jagoe *et al*, 2006; Shiba *et al*, 2006). We postulated that interactions with additional proteins might have a function in regulating FIP3 function and targeting to the cleavage furrow. Indeed, it was already demonstrated that in addition to Rab11, FIP3 binds to Arf6 (Shin *et al*, 1999, 2001; Hickson *et al*, 2003; Fielding *et al*, 2005). To identify additional FIP3-interacting proteins, we undertook a proteomic approach. To that end we generated a goat anti-FIP3 antibody (Supplementary Figure 1) and immunopurified FIP3 from HeLa cell lysates. Bands enriched in eluates from anti-FIP3 beads (Supplementary Figure 1D) were identified by μLC-MS/MS (for details see Materials and methods). Mass spectrometry revealed that Cyk-4 co-precipitated with FIP3 (Supplementary Figure 1E). To confirm this interaction and to test whether it is direct, we used glutathione bead pull-down assays. As shown in Figure 1A, recombinant purified 6His–FIP3 bound to GST–Cyk-4 but not GST beads. Interestingly, FIP4 (a class II FIP closely related to FIP3) also interacted with GST–Cyk-4 (Figure 1A). In contrast, the class I FIPs, Rip11/FIP5 and RCP/FIP1, did not bind to GST–Cyk-4 beads (Figure 1A), suggesting that Cyk-4 binding is a feature of class II FIPs (Prekeris, 2003). To further characterize the binding between FIP3 and Cyk-4, we incubated GST–Cyk-4 beads with varying concentrations of recombinant 6His–FIP3. As shown in Figure 1B, FIP3 binds to Cyk-4 with an apparent affinity of about 1 μM.

To determine the region of Cyk-4 that interacts with FIP3, we generated constructs of GST fused to either the N- or C terminus of Cyk-4 (Cyk-4-Nt and Cyk-4-GAP, respectively) (Figure 1C). Cyk-4-Nt contains the regions previously reported to bind to MKLP1 and ECT2, whereas the Cyk-4-GAP construct corresponds to the C terminus containing the GAP domain (Chalamalasetty *et al*, 2006). Using glutathione bead pull-down assays we found that 6His–FIP3 binds to GST–Cyk-4-Nt beads (Figure 1D). We also observed weak binding of FIP3 to the Cyk-4 GAP domain (data not shown). To further confirm FIP3 binding to Cyk-4-Nt, we incubated GST–Cyk-4 beads with 6His–FIP3 in the presence or absence of soluble Cyk-4-Nt, Cyk-4-GAP or both. As shown in Figure 1E, Cyk-4-Nt efficiently competed with full-length Cyk-4 for binding to FIP3. We also observed weak competition between Cyk-4-GAP and full-length Cyk-4 (Figure 1E). Thus, while the N terminus of Cyk-4 is clearly the main FIP3-binding site, FIP3 may also weakly interact with the GAP domain of Cyk-4.

Rab11 and Arf6 has no effect on FIP3 and Cyk-4 interaction

As class II FIPs also bind Rab11 and Arf6 GTPases (Fielding *et al*, 2005) we tested whether Rab11 or Arf6 can modulate the binding between FIP3 and Cyk-4. To that end, we incubated 6His–FIP3 with GST–Cyk-4 beads in the presence or absence of soluble Arf6 or Rab11 (Figure 2A). Neither Rab11 nor Arf6 modulated the binding of Cyk-4 to FIP3 (Figure 2A). This suggests that Cyk-4 interacts with a FIP3 region that may be distinct from the Rab11- and Arf6-binding motifs (Figure 2B). We and others have previously shown that FIP3(441–756) contains Rab11- and Arf6-binding domains (Figure 2B) (Fielding *et al*, 2005; Shiba *et al*, 2006; Schonteich *et al*, 2007). To test whether FIP3(441–756) can also bind Cyk-4, we incubated GST–Cyk-4 beads with 6His–FIP3 in the presence or absence of four-fold excess (as compared with 6His–FIP3) of FIP3(441–756) (hereafter FIP3-F1). FIP3-F1 competed with full-length 6His–FIP3 for binding to GST–Cyk-4 (Figure 2C), suggesting that the Cyk-4-binding motif is located within FIP3-F1. To further map the Cyk-4-binding domain we made a FIP3(610–756) truncation mutant (hereafter FIP3-F1a) fused to GST. This truncation deletes the predicted α-helix from the N terminus of FIP3-F1 (Figure 2B) and has no effect on Rab11 binding ((Eathiraj *et al*, 2006) and Figure 2D). In contrast, FIP3-F1a did not bind to GST–Cyk-4 beads, indicating that distinct regions of FIP3 interact with Cyk-4 as compared with Rab11 and Arf6 (Figure 2D).

FIP3 binds to Cyk-4 during late stage of cytokinesis

Cyk-4 binds to MKLP1, forming the centralspindlin complex (Mishima *et al*, 2002). During anaphase, centralspindlin is present at the mid-zone of dividing cells (Mishima *et al*, 2002). As cytokinesis progresses, centralspindlin gets

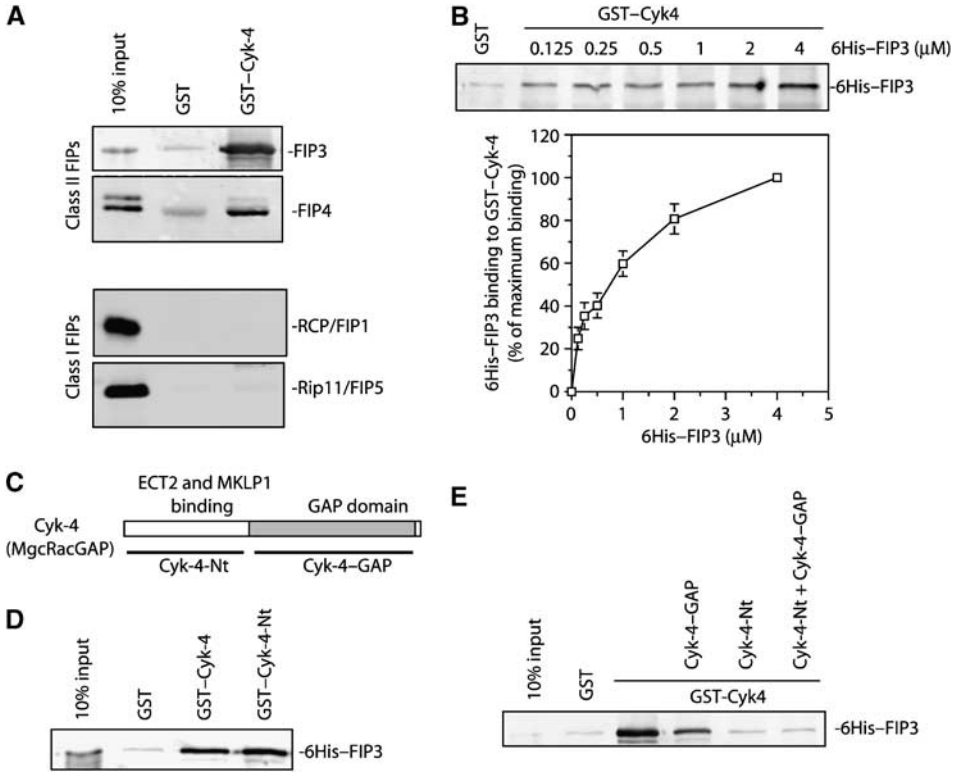

Figure 1 FIP3 is a Cyk-4-binding protein. (**A**) Glutathione beads coated with GST or GST–Cyk-4 incubated with recombinant 6His–FIP3, RCP, Rip11 or FIP4. The beads were washed and bound 6His–FIP3 was analysed by immunoblotting. (**B**) Glutathione beads coated with GST or GST–Cyk-4 incubated with varying concentrations of recombinant 6His–FIP3. The beads were washed and bound 6His–FIP3 was analysed by immunoblotting. The data shown are the means and standard errors calculated from four independent experiments. (**C**) Schematic representation of Cyk-4 truncation constructs used in Figures 1, 2 and 4. (**D**, **E**) GST, GST–Cyk-4 or GST–Cyk-4-Nt beads were combined with 6His–FIP3 in the presence or absence of soluble recombinant Cyk-4-GAP or Cyk-4-Nt. 6His–FIP3 binding was analysed by immunoblotting.

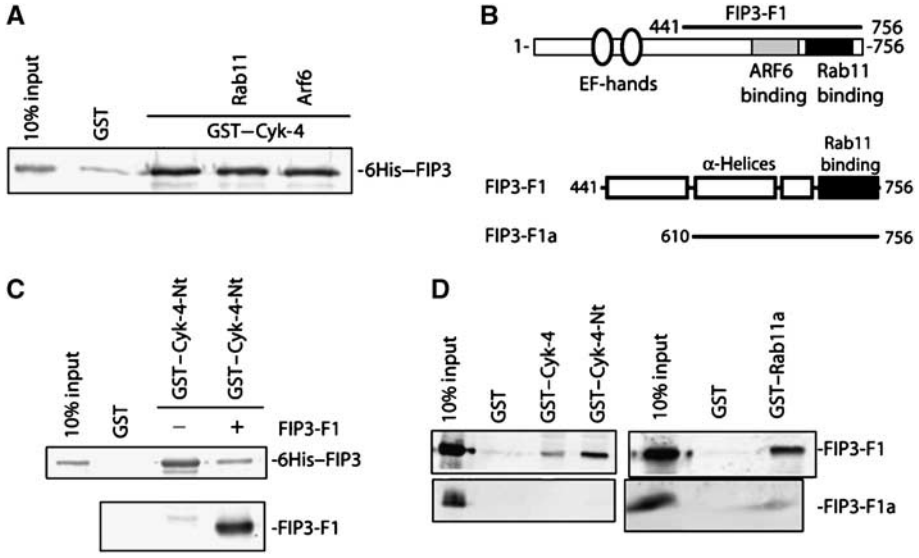

Figure 2 Identification of the Cyk-4-binding domain on FIP3. (**A**) Glutathione beads coated with GST or GST–Cyk-4 were incubated with soluble 6His–FIP3 in the presence or absence of five-fold excess of soluble Rab11–GTPγS or Arf6–GTPγS. The beads were washed and bound 6His–FIP3 was analysed by immunoblotting. (**B**) Schematic representation of various FIP3 truncation mutants used in the glutathione bead pull-down assays. (**C**) GST or GST–Cyk-4-Nt beads were incubated with 6His–FIP3 in the presence or absence of five-fold excess (mol/mol) of soluble recombinant FIP3-F1 fragment. (**D**) GST, GST–Cyk-4, GST–Cyk-4-Nt or GST–Rab11a beads were incubated with FIP3-F1 or FIP3-F1a fragments. The binding of FIP3 truncation fragments was analysed by immunoblotting with goat anti-FIP3 antibodies.

compacted and by late telophase is highly concentrated at the mid-body (Mishima *et al*, 2002). To test whether FIP3 and Cyk-4 (as part of centralspindlin) colocalize during mitosis, we analysed the distribution of FIP3 and Cyk-4 in HeLa cells at the different stages of mitosis (Figure 3A). To that end, we used a HeLa cell line stably expressing low levels of FIP3-GFP

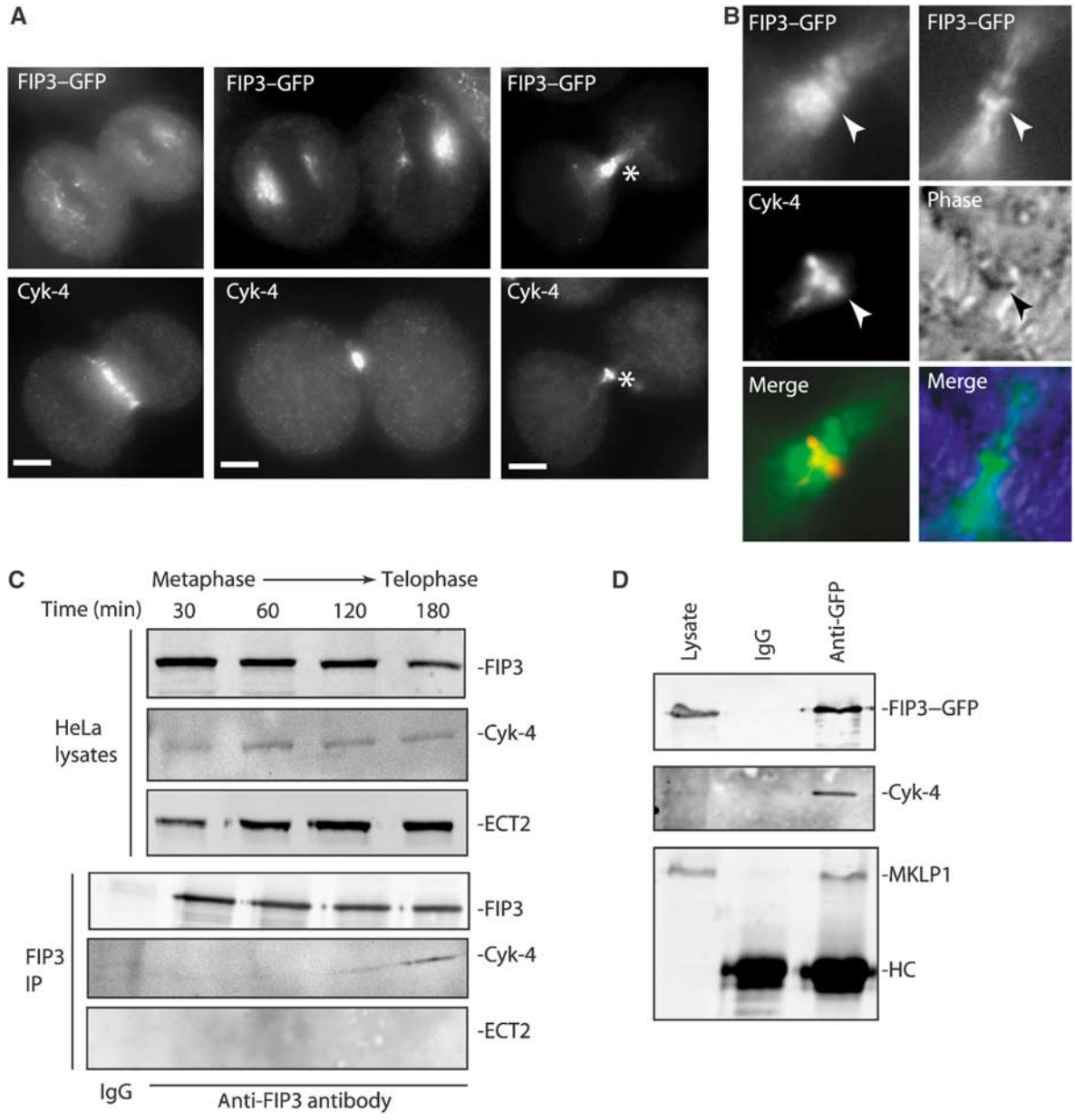

Figure 3 FIP3 associates with Cyk-4 during late stages of cytokinesis. (**A**) FIP3 and Cyk-4 colocalize at the mid-body during telophase. HeLa cells stably expressing GFP–FIP3 (top panels) were fixed and stained with anti-Cyk-4 antibodies (bottom panels). Asterisk marks the position of the mid-body. Panels from left to right show cells in anaphase, early telophase and late telophase, respectively. Bars 5 μm. (**B**) Higher magnification images of FIP3–GFP localization at the mid-body during late telophase. (**C**) HeLa cells synchronized using a double thymidine/nocodazole block were washed and harvested at various time points. FIP3 was then immunoprecipitated using anti-FIP3 antibodies. The immunoprecipitates, as well as starting lysates, were immunoblotted for the presence of FIP3, Cyk-4 and ECT2. (**D**) FIP3–GFP expressing stable HeLa cell line was synchronized using a double thymidine/nocodazole block and washed and incubated for 180 min. Cells were then lysed and FIP3–GFP was then immunoprecipitated using rabbit anti-GFP antibodies. Rabbit IgG was used as a negative control. The immunoprecipitates were immunoblotted for the presence of FIP3–GFP, Cyk-4 and MKLP1.

(about 1:2 compared with endogenous FIP3). We and others have previously shown that FIP3-GFP subcellular localization during mitosis closely mimics the localization of endogenous FIP3 (Hickson *et al*, 2003; Horgan *et al*, 2004; Fielding *et al*, 2005; Wilson *et al*, 2005; Schonteich *et al*, 2007). We also have shown that tagging FIP3 with GFP at C terminus has no effect on FIP3 binding to Rab11 or Arf6 (Fielding *et al*, 2005; Wilson *et al*, 2005). Thus, it is very likely that FIP3–GFP closely mimics the properties of endogenous FIP3 during mitosis. As previously reported, during anaphase and early telophase FIP3–GFP was associated with centrosomes with no detectable FIP3–GFP at the mid-zone (Wilson *et al*, 2005). At early telophase, FIP3–GFP-containing endosomes moved to the furrow just outside the mid-body (Fielding *et al*, 2005; Wilson *et al*, 2005). Finally, at late telophase FIP3–GFP moved to the mid-body, although some FIP3–GFP could still be observed on each side of the furrow (Figure 3A and B) (Fielding *et al*, 2005; Wilson *et al*, 2005). FIP3–GFP colocalized with Cyk-4 only at late telophase, suggesting that FIP3 binds to Cyk-4 only at a very late stage of cytokinesis, perhaps just before or during abscission (Figure 3A and B; also see Figure 7A).

To confirm that FIP3 binds to Cyk-4 at late telophase, we immunoprecipitated endogenous FIP3 from synchronized HeLa cells at different stages of mitosis (for synchronization efficiency, see Supplementary Figure 2). Whereas the levels of Cyk-4 and FIP3 did not dramatically change during cytokinesis, Cyk-4 co-precipitated with endogenous FIP3 only at late telophase (Figure 3C and Supplementary Figure 2). Interestingly, we could not detect any ECT2 co-precipitating with FIP3 (Figure 3C), suggesting that FIP3 and ECT2 may form mutually exclusive complexes with centralspindlin. To further confirm that FIP3 binds to centralspindlin complex, we immunoprecipitated FIP3–GFP (from HeLa cells stably expressing FIP3–GFP) using anti-GFP antibodies from synchronized cells at late telophase (180 min after release from nocodazole block). As shown in the Figure 3D, both centralspindlin complex members, Cyk-4 and MKLP1, co-immunoprecipitated with FIP3–GFP at late telophase.

Centralspindlin is required for the recruitment of FIP3 to the mid-body

Our data are consistent with the possibility that Cyk-4 recruits FIP3 to the mid-body. To investigate the role of endogenous centralspindlin in FIP3 targeting, we treated HeLa cells stably expressing FIP3–GFP with MKLP1 siRNA. As shown in Figure 4, in cells depleted of MKLP1, FIP3 initially concentrated around the spindle poles and subsequently localized to the mid-body side of the nucleus, but this was transient and FIP3 failed to accumulate at the mid-body (Figure 4, right panels). Aurora B kinase phosphorylation of MKLP1 is required for abscission during late telophase (Guse *et al*, 2005). As expected, Aurora B depletion similarly prevented accumulation of FIP3 at the mid-body (Supplementary Figures 5 and 6). We also tested whether FIP3 may be required for the formation and targeting of the centralspindlin complex. We depleted FIP3 and assessed the localization of Cyk-4 and

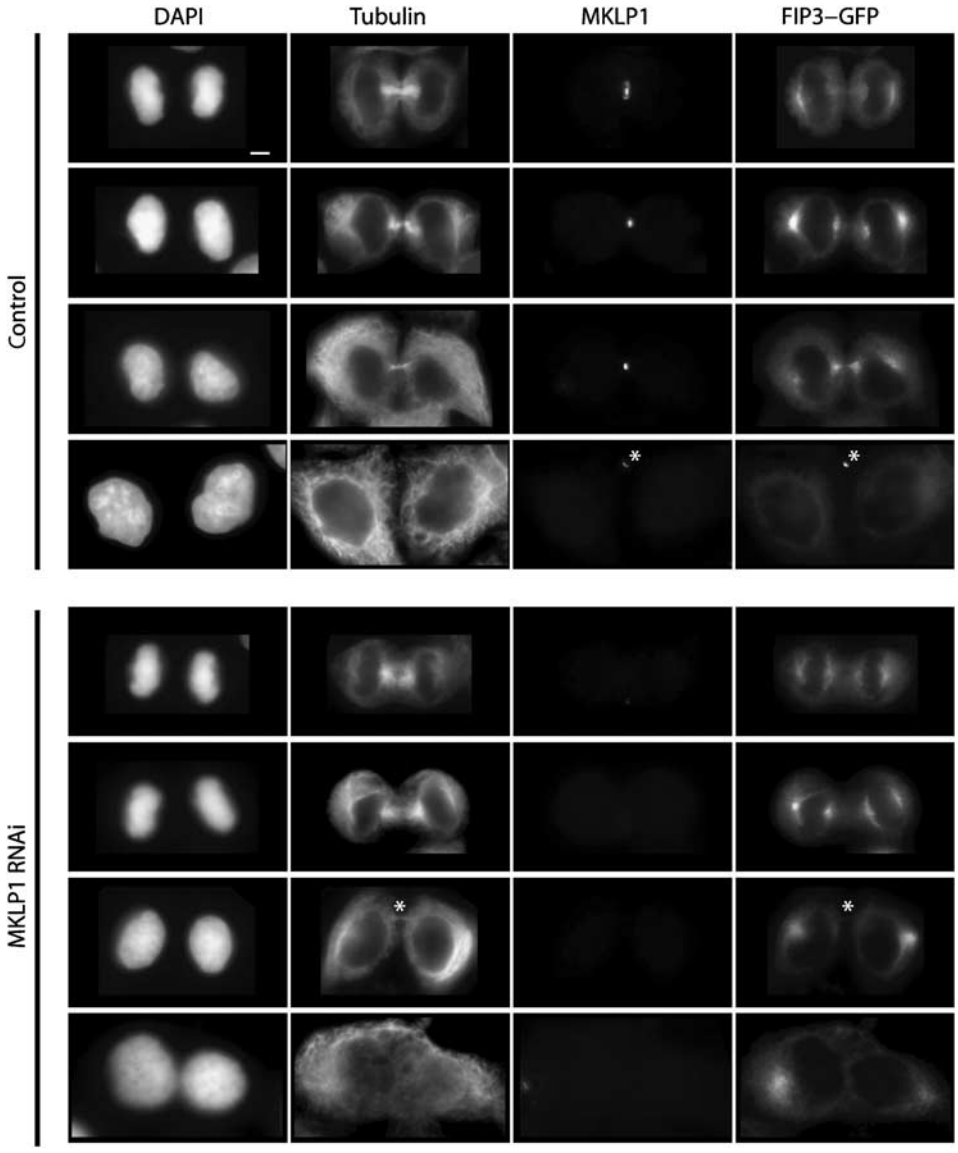

Figure 4 MKLP1 is necessary for FIP3 recruitment to the cleavage furrow of mitotic cells. HeLa cells expressing FIP3–GFP were either mock transfected (top panels) or transfected with MKLP1 siRNA (bottom panels). Cells were fixed and stained with anti-tubulin and anti-MKLP1 antibodies. Asterisks mark the mid-bodies. Size bar 10 μm.

ECT2 in dividing HeLa cells. As shown in Supplementary Figure 3, FIP3 siRNA had no effect on the localization of Cyk-4 and ECT2 during cytokinesis.

The dynamics of FIP3-containing endosomes during cell division

The data presented here suggest that Cyk-4 binding mediates the targeting of FIP3-containing endosomes to the mid-body at late telophase. Although this hypothesis explains the accumulation of FIP3 at the mid-body, the mechanisms responsible for moving FIP3-containing endosomes to the cleavage furrow remain unclear. One possibility is that recycling endosomes continuously move in and out of the cleavage furrow and only accumulate at the mid-body upon binding to the centralspindlin complex. Alternatively, recycling endosomes could synchronously and directionally move to the mid-body at late telophase. To investigate these models, we used time-lapse microscopy to follow the distribution of FIP3–GFP in dividing HeLa cells during mitosis (Figure 5A). In early and mid-telophase cells, we observed FIP3–GFP-containing endosomes moving to and from the cleavage furrow (Figure 5B, C, F and G; Supplementary movie 1). This movement is likely dependent on mid-zone microtubules as FIP3–GFP colocalizes with microtubules (Fielding *et al*, 2005; Wilson *et al*, 2005) and nocodazole treatment resulted in inhibition of the FIP3–GFP motility (data not shown). Interestingly, the majority of FIP3–GFP-containing organelles moved towards the furrow (65.2%; see Figure 5), thus resulting in gradual accumulation of the FIP3–GFP in the vicinity of the mid-body.

To further understand the dynamics of FIP3-containing endosomes, we analysed FIP3–GFP expressing HeLa cells using fluorescence recovery after photobleaching (FRAP) and fluorescence loss in photobleaching (FLIP). First, we bleached FIP3–GFP-containing endosomes at one side of the furrow and analysed the recovery of its fluorescence,

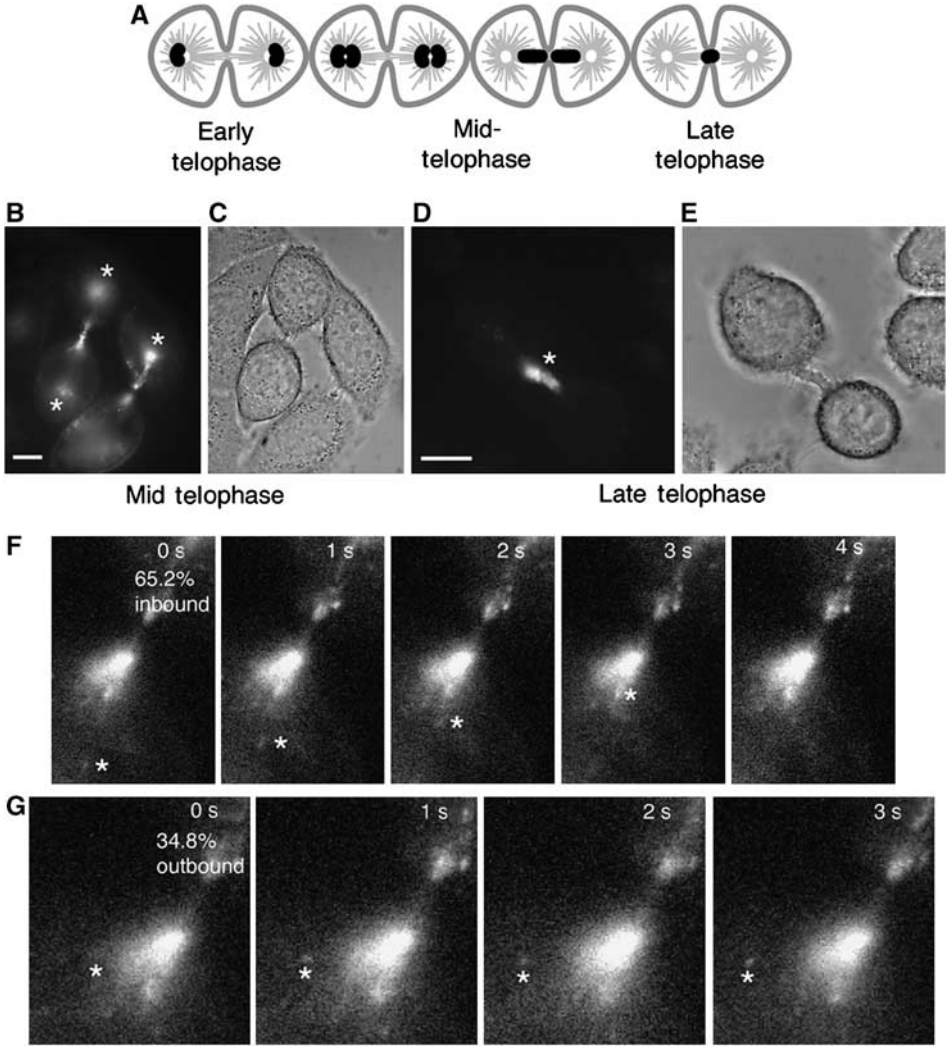

Figure 5 The dynamics of FIP3-containing endosomes during telophase. (**A**) The schematic representation of FIP3 localization during early, mid- and late telophase. (**B–E**) HeLa cells stably expressing FIP3–GFP at mid- (B, C) or late (D, E) telophase were imaged by time-lapse microscopy. Asterisks in (B) mark centrosomally associated FIP3–GFP. Asterisk in (D) marks mid-body. Size bar 2 μm. For entire time-lapse series, see Supplementary movies 1 and 2. (**F**, **G**) Higher magnification sets of sequential images from the time-lapse series of a FIP3–GFP-expressing cell in mid-telophase. Asterisks mark FIP3–GFP-containing organelle that either move to (F) or from (G) cleavage furrow. The number shown in (F,G) is the percentage of organelles moving to (inbound) or from (outbound) mid-body (total 93 organelles from 5 cells analysed).

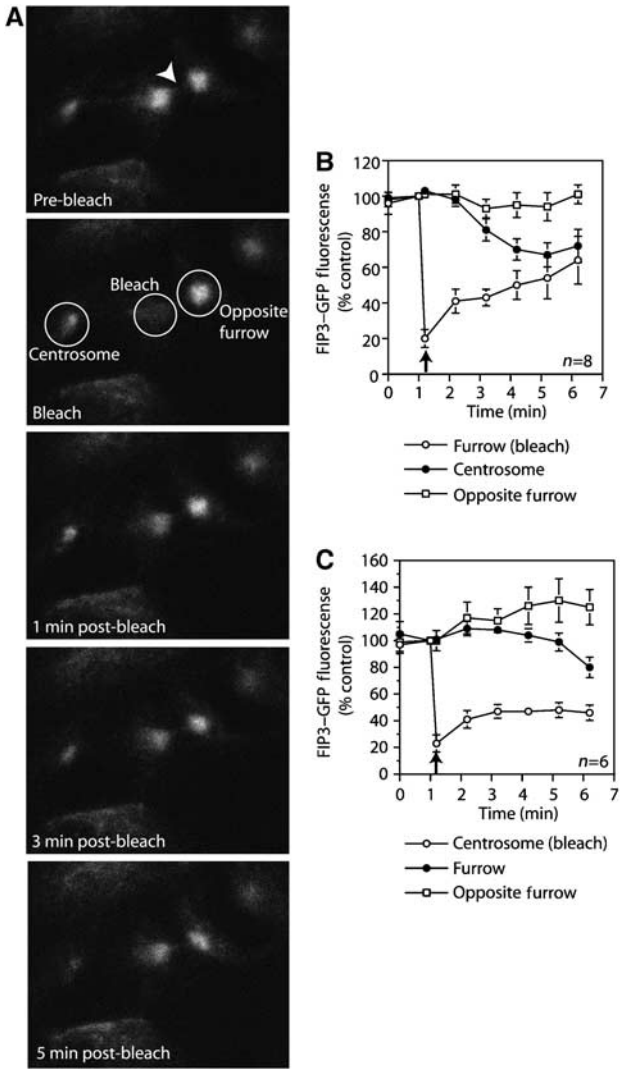

Figure 6 FRAP analysis of FIP3–GFP dynamics during early telophase. To analyse the dynamics of FIP3–GFP-containing endosomes at early telophase, fluorescent recovery after photobleaching (FRAP) of furrow (**A**, **B**) or centrosome (**C**) associated FIP3–GFP was carried out in HeLa cells. Circles in (A) mark the areas analysed before and after photobleaching. Arrowhead in (A) marks the furrow of the dividing cells. (B) The quantitation of furrow-associated FIP3–GFP FRAP analysis. The data shown are the means and standard errors from derived from eight randomly chosen cells. (C) The quantitation of centrosome-associated FIP3–GFP FRAP analysis. The data shown are the means and standard errors derived from six randomly chosen cells.

while also monitoring the fluorescence of the FIP3–GFP associated with centrosome on the same side of the cell and furrow on the opposite side of the cell (Figure 6A). As shown in Figure 6A and B, the fluorescence of the furrow-associated FIP3–GFP rapidly recovered after photobleaching. During the same period of time the fluorescence of centrosomal FIP3–GFP decreased with the similar rate, suggesting that unbleached FIP3–GFP-containing endosomes moved from centrosome to the furrow (Figure 6A and B). In contrast, the fluorescence of FIP3–GFP associated with opposite side of the furrow did not change, indicating that endosomes do not exchange between daughter cells during telophase (Figure 6A and B). To determine whether FIP3–GFP endosomes also return to the centrosome from the furrow, we bleached centrosomal FIP3–GFP and measured the rate of its recovery and fluorescence loss of furrow-associated FIP3 (on both sides of the mid-body). As shown in the Figure 6C, centrosome-associated FIP3–GFP recovered partially after photobleaching (compare Figure 6B and C). The limited recovery of FIP3–GFP is likely due to the fact that during the recovery period cell continued progressing towards late telophase, resulting in overall accumulation of FIP3–GFP at the furrow. In addition, we only observed loss in fluorescence of furrow FIP3–GFP at the late stages of the recovery (last couple of minutes), suggesting that the transport of FIP3–GFP endosomes from the furrow to centrosome is less efficient and only partially responsible for the recovery of centrosomal FIP3–GFP. That is consistent with time-lapse data showing that FIP3–GFP-containing organelles moved towards the furrow at higher frequency the away from the furrow (see Figure 5).

In contrast to FIP3–GFP dynamics at early telophase, during late telophase FIP3–GFP accumulated around the mid-body and exhibited little movement (Figure 5D and E; Supplementary movie 2), suggesting that during late mitosis FIP3–GFP-containing endosomes become trapped in or tethered to the mid-body. Thus, based on all our data we hypothesize that FIP3 binding to Cyk-4 may serve as tether that 'captures' FIP3-containing endosomes and concentrates them at the mid-body in late telophase.

ECT2 regulates FIP3 recruitment to the mid-zone during cytokinesis

The interaction between the N termini of Cyk-4 and ECT2 results in the accumulation of ECT2 to the mid-zone during cytokinesis (Yuce *et al*, 2005). Our data demonstrate that FIP3 also binds to the N terminus of Cyk-4 (see Figure 1). Furthermore, the N terminus of Cyk-4 also binds to MKLP1 and ECT2 (Yuce *et al*, 2005). As the interaction between centralspindlin components is required for their mid-body localization (Jantsch-Plunger *et al*, 2000; Mishima *et al*, 2002) Cyk-4 should be able to bind MKLP1 and FIP3 simultaneously. To test this, we incubated GST–Cyk-4 beads with soluble 6His–FIP3 in the presence or absence of varying concentrations of MKLP1(445–620), the domain that is known to bind Cyk-4. As shown in Figure 7A, MKLP1(445–620) had no effect on the interaction of FIP3 and Cyk-4-Nt, suggesting that MKLP1 does not inhibit FIP3 binding to Cyk-4.

Our immunoprecipitation studies suggested that ECT2 and FIP3 may form a mutually exclusive complexes with Cytk-4 (Figure 3B). To test whether ECT2 may directly affect the FIP3 and Cyk-4 interaction, we incubated GST–Cyk-4 beads with 6His–FIP3 in the presence or absence of varying concentrations of ECT2(1–333) (hereafter ECT2-N), the domain previously shown to bind Cyk-4 (Yuce *et al*, 2005; Chalamalasetty *et al*, 2006). Interestingly, ECT2-N efficiently inhibited FIP3 binding to Cyk-4 (Figure 6A and B), suggesting that ECT2 and FIP3 form mutually exclusive complexes with Cyk-4. Furthermore, at equimolar 6His–FIP3 and ECT2-N ratio, 6His–FIP3 binding to GST–Cyk-4 was inhibited to about 50%, suggesting that FIP3 and ECT2 bind to Cyk-4 with similar affinities (Figure 7B). These data are also consistent with our previous data showing that ECT2 does not co-precipitate with FIP3 at late telophase (Figure 3).

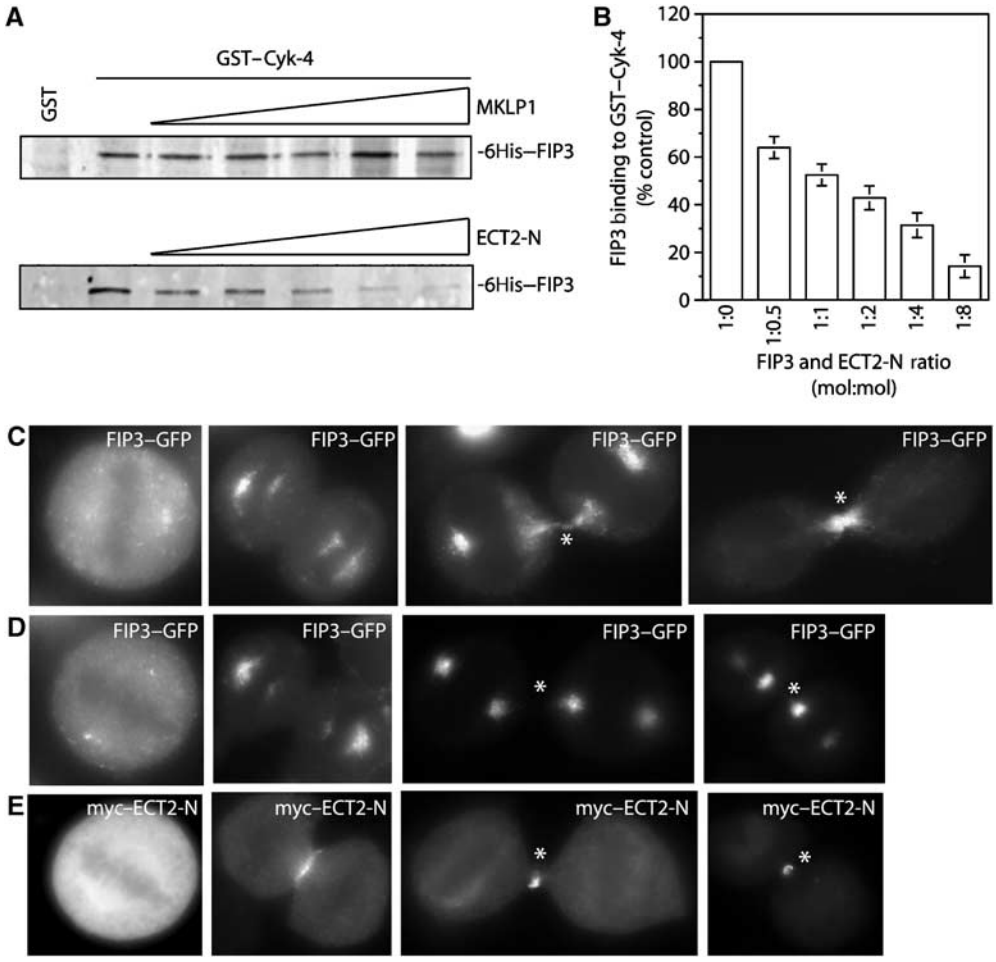

Figure 7 ECT2 inhibits FIP3 binding to centralspindilin. (**A**, **B**) GST or GST–Cyk-4 beads were incubated with 6His–FIP3 in the presence or absence of varying concentrations (from 1:0.5 to 1:8 mol/mol ratio) of recombinant soluble MKLP1 (A) or ECT2-N (B). Beads were then washed and bound 6His–FIP3 was analysed by immunoblotting. Data shown in (B) are the means and standard errors calculated from three different experiments. (**C**–**E**) HeLa cells expressing FIP3–GFP alone (C) or expressing FIP3–GFP and myc–ECT2-N (D, E) were fixed and stained with anti-myc antibodies (E). Asterisks mark mid-bodies.

The competition between FIP3 and ECT2 for binding to Cyk-4 raises the possibility that ECT2 may inhibit FIP3 binding to the centralspindlin complex. Indeed, it was reported that ECT2-N overexpression in mammalian cells inhibits abscission (Chalamalasetty *et al*, 2006), which phenotypically resembles FIP3 depletion (Wilson *et al*, 2005). We transfected HeLa cells with myc–ECT2-N and examined whether this perturbation inhibits FIP3 localization at different stages of mitosis. As shown in Figure 7C–E, FIP3–GFP localization in metaphase and anaphase was not affected by expression of myc–ECT2-N. As previously reported, FIP3–GFP accumulated around centrosomes during anaphase (Fielding *et al*, 2005; Wilson *et al*, 2005; also see Figures 3, 5 and 8). During early telophase, in control cells FIP3–GFP started moving and slowly accumulating in the furrow, presumably via mid-zone microtubules (Figure 7C). In contrast, in myc–ECT2-N-expressing cells, FIP3–GFP was associated with mid-zone microtubules, but FIP3–GFP did not accumulate in the furrow (Figure 7D and E). Finally, while in control cells at late telophase FIP3–GFP has moved to the furrow/mid-body, in myc–ECT2-N-expressing cells, while FIP3–GFP has moved away from centrosomes, FIP3–GFP remained excluded from the furrow and mid-body (no mid-body localization was observed in 120 randomly chosen mitotic cells at late telophase) (Figure 7D and E). A similar effect of myc–ECT2-N overexpression on endogenous FIP3 localization was also observed (data not shown).

Our data suggest that ECT2 binding to Cyk-4 blocks the ability of FIP3 to bind to centralspindlin. If this were true and most of the Cyk-4 molecules were bound to ECT2, then ECT2 would be predicted to dissociate from Cyk-4 before FIP3 can accumulate at the mid-body. To test this hypothesis, we stained HeLa cells stably expressing FIP3–GFP at the different stages of mitosis with anti-ECT2 and anti-Cyk-4 antibodies. As reported previously (Yuce *et al*, 2005; Nishimura and Yonemura, 2006), ECT2 accumulates at the mid-zone and mid-body during anaphase and early telophase (Figure 8A). However, during mid-telophase, ECT2 staining at the mid-body begins to decline, although the levels of Cyk-4 remained unchanged (Figure 8A and C). It was previously reported that removal of ECT2 from the mid-zone coincides with reformation of the nucleus and nuclear import of ECT2 (Saito *et al*, 2004; Chalamalasetty *et al*, 2006). Quantitation of ECT2 and FIP3 levels in numerous cells indicate that FIP3 recruitment occurs subsequent to the reduction in ECT2 levels (Figure 8C).

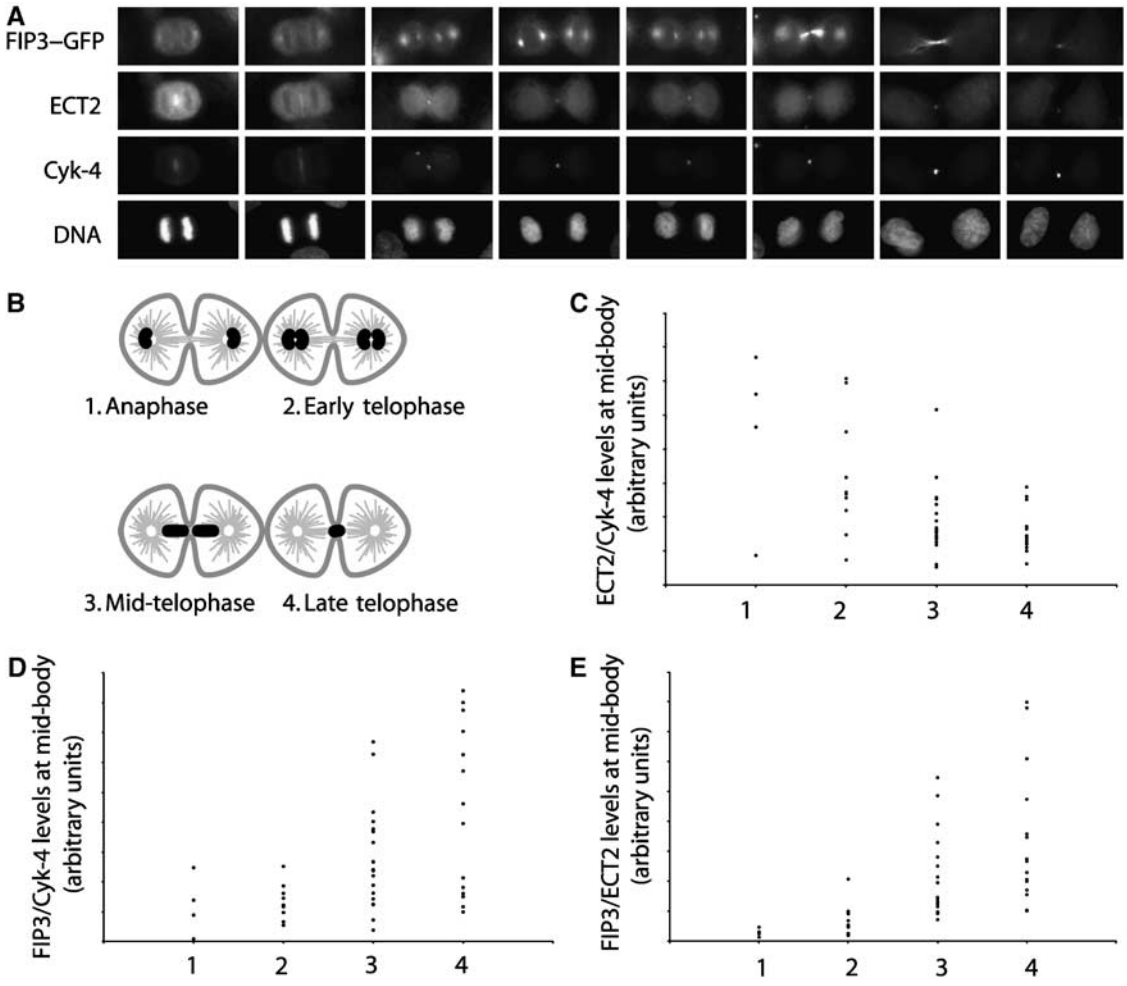

Figure 8 FIP3 and ECT2 are sequentially recruited to the mid-body. (**A**) HeLa cells stably expressing FIP3–GFP were fixed and stained with anti-ECT2 and anti-Cyk-4 antibodies as well as Hoechst. Images from left to right display cells at various stages of mitosis. (**B**) The schematic representation of FIP3 localization during anaphase, early, mid- and late telophase. (**C**–**E**) FIP3–GFP-expressing cells were classified into four categories (see B). The ratiometric analysis of the levels of ECT2, Cyk-4 and FIP3–GFP at the mid-body of randomly chosen cells was completed as described in Materials and methods. The data were expressed as ratios between ECT2/Cyk-4, FIP3–GFP/Cyk-4 and FIP3–GFP/ECT2.

To further examine the relationship between ECT2 and FIP3, we examined how FIP3 responds to knock down of ECT2 by siRNA. If FIP3 and ECT2 simply compete, ECT2 depletion would be expected to result in the premature accumulation of FIP3 at the mid-zone during early cytokinesis. Previously published data have shown that FIP3 accumulates around centrosomes and only translocates to the cleavage furrow at late telophase after the complete ingression of the furrow and mid-body formation (Fielding *et al*, 2005; Wilson *et al*, 2005). At the beginning, a small amount of FIP3 could be observed near DNA on the opposite side of centrosomes (Supplementary Figure 4), where it colocalizes with the minus ends of mid-zone microtubules (data not shown). During ingression, FIP3 gradually moves from the centrosomes to mid-zone microtubules and eventually translocates to the mid-body (Figure 8A and Supplementary Figure 4). Inhibition of furrowing with blebbstatin prevents this translocation, thus arresting FIP3 with the early anaphase distribution (Supplementary Figure 4). Interestingly, whereas ECT2 knockdown also inhibited furrowing, it did not block FIP3 translocation to the mid-zone microtubules. In ECT2-depleted cells, little FIP3 remained associated with centrosomes and the majority of FIP3 colocalized with mid-zone microtubules (Figure 9). However, this pattern of FIP3 localization is distinct from that of centralspindlin, in particular, precocious FIP3 localization to the central spindle was not observed (data not shown). These data indicate that although ECT2 influences FIP3 dynamics during cytokinesis, other proteins that are recruited to the mid-body during furrowing may also have a function in FIP3 targeting. For instance, the exocyst complex and Arf6 were also implicated in regulating FIP3 recruitment to the mid-body (Fielding *et al*, 2005). Together with the data in Figure 7, we suggest that ECT2 delocalization is necessary, but not sufficient to recruit FIP3 to the mid-body.

Discussion

Endocytic membrane traffic is critical for cytokinesis in animal cells (Shuster and Burgess, 2002; Riggs *et al*, 2003). The targeting of recycling endosomes to the cleavage furrow likely delivers membranes required for abscission during cell division (Wilson *et al*, 2005). Furthermore, endocytic membrane transport contributes to actin dynamics, as well as to

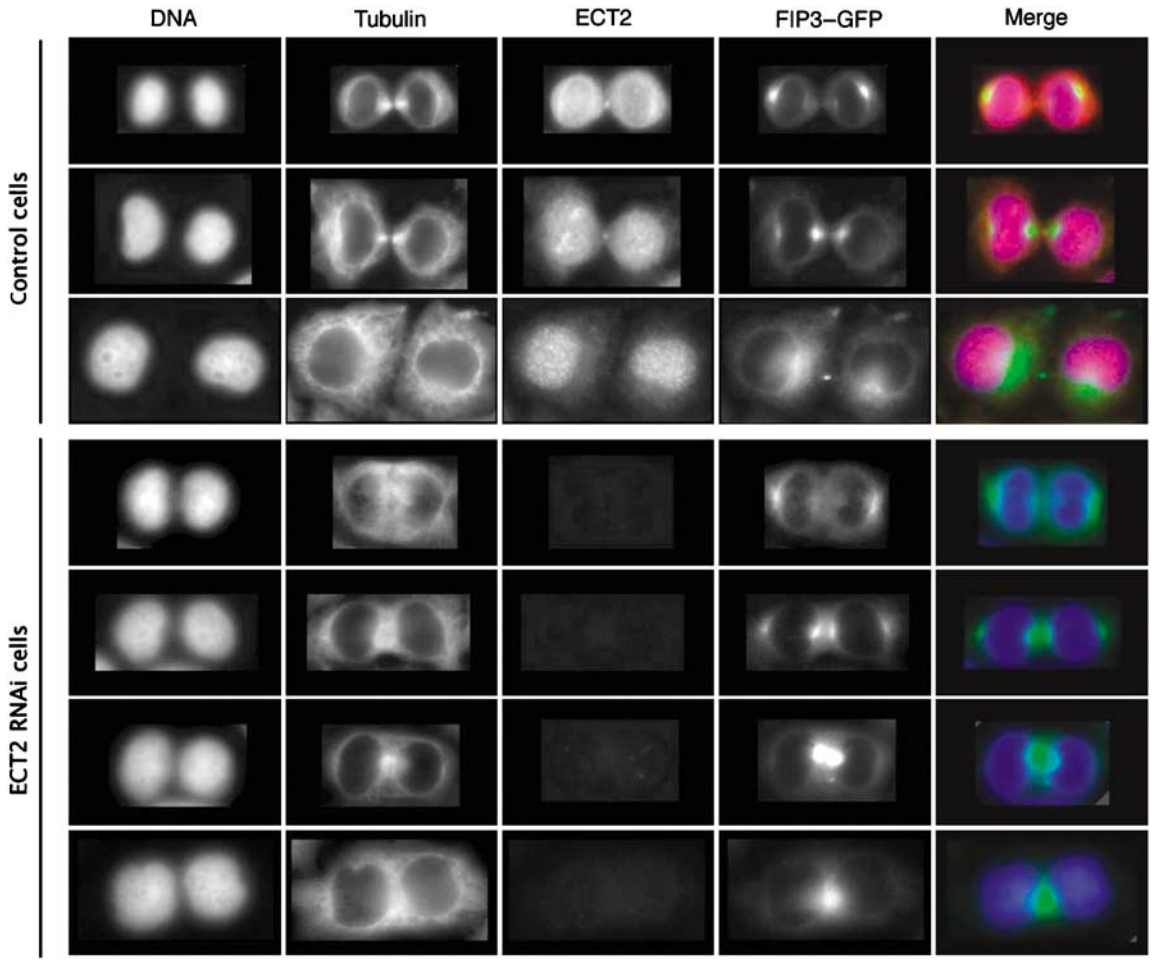

Figure 9 ECT2 knockdown enhances FIP3 translocation to the mid-zone. HeLa cells stably expressing FIP3–GFP were either mock treated (control) or transfected with ECT2 siRNA. Cells were fixed and stained with anti-ECT2 and anti-tubulin antibodies as well as Hoechst. Images display cells at various stages of cytokinesis.

modulation of membrane lipids at the cleavage furrow (Riggs *et al*, 2003; Janetopoulos *et al*, 2005). Targeting of recycling endosomes to the cleavage furrow is mediated by Rab11 and Rab35 GTPases, members of the Rab family of Ras-like small monomeric GTPases (Prekeris *et al*, 2000, 2001; Kouranti *et al*, 2006; Hales *et al*, 2001). Rab11 functions by recruiting FIP proteins to membranes (Hickson *et al*, 2003). FIP3, a FIP family member, regulates the temporal and spatial dynamics of the recycling endosome during cytokinesis (Wilson *et al*, 2005), although the molecular machinery of FIP3 action remains to be fully understood. Here, we demonstrate that FIP3 binds to the centralspindlin component Cyk-4/MgcRacGAP. Centralspindlin is well known for its role in the regulation of cleavage furrow through the recruitment of the RhoA GEF ECT2 to the mid-zone (Yuce *et al*, 2005; Nishimura and Yonemura, 2006). Our data suggest that the centralspindlin complex may have an additional function, namely to mediate recycling endosome targeting to the mid-body during abscission.

The dynamics of FIP3-containing recycling endosomes is tightly controlled during mitosis. At early anaphase, FIP3-containing endosomes accumulate around the centrosomes, where they stay until the end of furrow ingression (Horgan *et al*, 2004; Wilson *et al*, 2005). During anaphase, FIP3-containing endosomes partition to the furrow side of the nucleus, likely at the minus ends of the mid-zone microtubule bundles. At late telophase, FIP3-containing endosomes move to furrow where they accumulate at the mid-body of dividing cells (Wilson *et al*, 2005). The targeting of FIP3 and recycling endosomes to the mid-body appears to be a requirement for successful abscission (Wilson *et al*, 2005). Interestingly, our time-lapse and FRAP analyses have shown that FIP3-containing endosomes are dynamic during early and mid-telophase, and continuously move in and out of the mid-body region. The motility appears to be dependent on microtubules, as FIP3 colocalizes with microtubules and the microtubule depolymerizing agent nocodazole inhibits FIP3 movement to the cleavage furrow (Horgan *et al*, 2004; Wilson *et al*, 2005). At late telophase, the motility of FIP3-containing endosomes is dramatically reduced likely causing FIP3 to accumulate at the mid-body. Thus, we propose that centralspindlin does not transport recycling endosomes but rather works as a tethering factor that 'captures' FIP3-containing endosomes during late telophase.

The observation that FIP3-containing endosomes can enter the cleavage furrow even at early telophase raises the question whether Cyk-4 is 'available' for FIP3 binding only at late telophase, as we do not observe association of FIP3 with the mid-body until this stage of mitosis. We have shown that ECT2 and FIP3 competitively bind to overlapping regions of

Cyk-4. As ECT2 is recruited to the centralspindlin at metaphase/early anaphase, it could prevent FIP3 from binding to Cyk-4 in early mitosis. Indeed, overexpression of myc–ECT2(1–333) inhibits the recruitment of FIP3 to the mid-body, presumably by blocking its binding to Cyk-4. This result is consistent with published data showing that this ECT fragment inhibits abscission independently of its effects on RhoA activation (Chalamalasetty *et al*, 2006). We also showed that delocalization of ECT2 from the mid-body at late telophase precedes the recruitment of FIP3 to the mid-body. Collectively, such data argue that the interaction of Cyk-4 with ECT2 has a potential to limit the availability of Cyk-4 for FIP3 binding.

FIP3 does not appear to direct the removal of ECT2 at late telophase, as FIP3 knockdown (Supplementary Figure 3) or overexpression (data not shown) does not affect the distribution of ECT2 in mitotic cells. However, dissociation of ECT2 precedes FIP3 recruitment to the mid-body. At late telophase, ECT2 is sequestered into reforming nuclei freeing Cyk-4 to interact with FIP3. Indeed, mutations in the ECT2 nuclear localization signal results in increased association of ECT2 with the mid-body at late telophase and inhibits abscission (Chalamalasetty *et al*, 2006). Consistent with this model, nuclear envelope reformation correlates with FIP3 targeting to the cleavage furrow (Figure 8). We note, however, that knock down of ECT2 does not cause premature association of FIP3 with centralspindlin at anaphase or early telophase, suggesting that other mechanisms may also regulate FIP3 binding to Cyk-4 *in vivo*.

In summary, we propose that the sequential binding of Cyk-4 to ECT2 and FIP3 regulates the targeting of recycling endosomes to the mid-body during mitosis. During anaphase and early telophase, ECT2 is bound to Cyk-4 where it regulates acto-myosin contractile ring (Figure 10A, steps 2 and 3). During this time, FIP3-containing recycling endosomes can move in and out of the cleavage furrow but fail to accumulate at the mid-zone due to ECT2 binding to Cyk-4 (Figure 10A, step 1). At late telophase, ECT2 dissociates from centralspindlin and relocates to the newly formed nuclei (Figure 10B, step 4). The removal of ECT2 then allows FIP3 to bind Cyk-4, thus resulting in the tethering of recycling endosomes to the mid-body (Figure 10B, step 5). Simultaneously, the tethering of FIP3 endosomes to the mid-body is also enhanced by the accumulation of the exocyst complex (see below) (Figure 10).

Although our data suggest the involvement of centralspindlin in targeting FIP3-containing recycling endosomes to the cleavage furrow, it is likely that other proteins regulate endosomal dynamics during mitosis. Indeed, several studies have implicated other molecules, such as Arf6 GTPase, centriolin and the exocyst complex in targeting membranes to the cleavage furrow (Schweitzer and D'Souza-Schorey, 2002, 2005; Low *et al*, 2003; Fielding *et al*, 2005; Gromley *et al*, 2005; Wilson *et al*, 2005). Interestingly, Arf6 has been shown to bind to both FIP3 (Figure 10B, step 5) and the exocyst complex (via the Sec10 subunit) (Prigent *et al*, 2003; Fielding *et al*, 2005). The Sec15 subunit of the exocyst is also known to bind Rab11 (Zhang *et al*, 2004). Finally, centriolin was also shown to bind to the Sec5 and Sec8 subunits of exocyst (Gromley *et al*, 2005). Although the requirement of all of these interactions in targeting recycling endosomes to the cleavage furrow remains to be fully understood, it is likely that multiple interactions redundantly ensure the specificity of membrane targeting (Figure 10, step 5). Consistent with this, knock down of Rab11 and Arf6 synergistically inhibits cytokinesis (Fielding *et al*, 2005; Wilson *et al*, 2005; Yu *et al*, 2007). This notion is also supported by our data showing that ECT2 knockdown alone is not sufficient to fully induce the translocation of FIP3 to the centralspindlin complex during anaphase. Thus, the simultaneous interactions of the FIP3/Rab11 complex with centralspindlin, Arf6 and the exocyst complex may ensure the spatial and temporal coordination of endosome recruitment to the mid-body during cytokinesis.

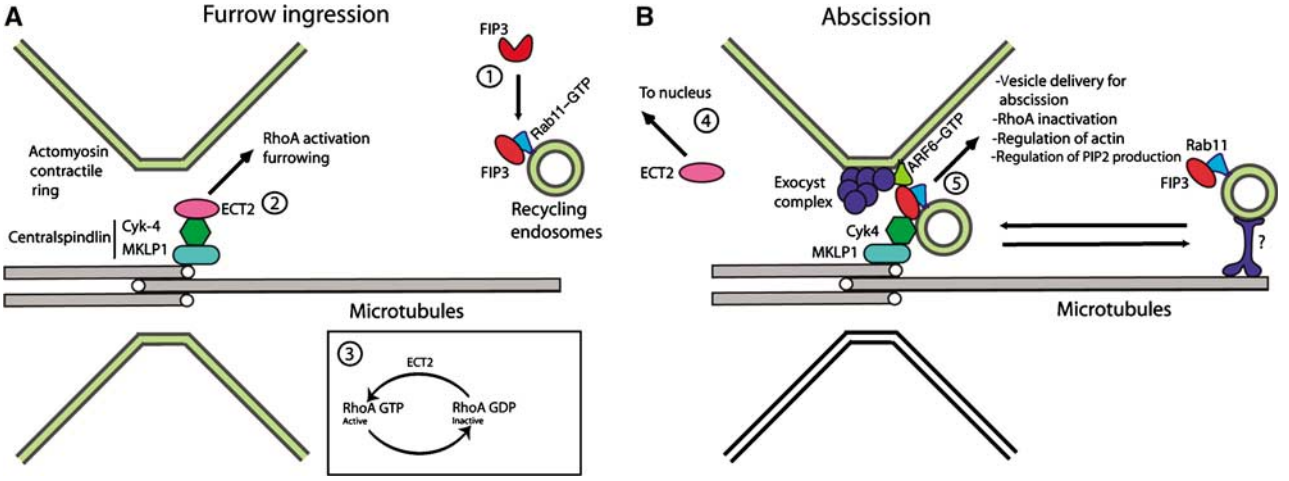

Figure 10 Model of FIP3 targeting to the cleavage furrow. Schematic representation of cells during anaphase (**A**) and late telophase (**B**). FIP3 is recruited to endosomes by binding to activated (GTP bound) Rab11 (step 1). During anaphase, ECT2 remains associated with centralspindlin complex (step 2) where it activates RhoA (step 3). During telophase FIP3-containing endosomes are delivered to the cleavage furrow through as yet unidentified motors (step 4). In late telophase, ECT2 disassociates from the centralspindlin complex and is sequestered to the reforming nucleus. The removal of ECT2 enables FIP3 to associate with Cyk-4 (step 5). Note that in addition to Cyk-4 binding, FIP3 also associates with Arf6 and the exocyst complex (indirectly) (step 5). Thus, the recruitment of FIP3-containing recycling endosomes is co-mediated by at least two tethering complexes, the exocyst and Cyk-4/MKLP1.

Materials and methods

Antibodies

Rabbit anti-ECT2, rabbit anti-MKLP1, rabbit anti-Cyk-4/MgcRacGAP, rabbit anti-MKLP1, rabbit anti-FIP3, goat anti-FIP3, rabbit anti-Rip11/FIP5 and rabbit anti-RCP/FIP1 antibodies were previously described (Prekeris *et al*, 2000; Kitamura *et al*, 2001; Mishima *et al*, 2002; Peden *et al*, 2004; Wilson *et al*, 2005; Yuce *et al*, 2005). Sheep anti-FIP4 antibody was previously described (Hickson *et al*, 2003). Mouse anti-β-tubulin antibody was purchased form BD Pharmingen (San Jose, CA). Mouse anti-Myc and anti-cyclin B antibodies were obtained from Santa Cruz Biotechnology (Santa Cruz, CA). Secondary antibodies conjugated to either fluorescein or Texas Red were purchased from Jackson ImmunoResearch Inc. (West Grove, PA). The Zenon system (Invitrogen, Carlsbad, CA) was used for co-labeling of Cyk-4 and ECT2. Cell-permeant Hoechst DNA stain was obtained from Invitrogen.

Proteomics

HeLa cell lysates from 20 10-cm plates were incubated overnight with either 20 μg/ml of goat anti-FIP3 antibodies or purified nonspecific goat IgG, followed by addition of 100 μl of protein G-sepharose/1 ml. Beads were then washed, resuspended in SDS–PAGE buffer, and separated on a 9–16% gradient acrylamide gel. The resulting gel was Coomassie stained and bands present only in anti-FIP3 immunoprecipitate were isolated. Gel bands were cut in three equal sections and in-gel digested using three proteases. Peptides were extracted from the gel pieces with 0.1% TFA/60% acetonitrile and lyophilized. Dried peptide samples from each gel band were rehydrated and loaded onto a microcapillary column (100 μm inner diameter fused silica) packed with 15 cm Aqua C18 reverse-phase material and then placed in-line with an LTQ linear trap mass spectrometer. Peptides were eluted with 2 h mobile gradient of acetonitrile/0.1% formic acid. Tandem mass spectra were analysed using Sequest using a human-mouse-rat database concatenated to a randomized human–mouse–rat database. DTASelect was used to reassemble identified peptides into proteins. Identified proteins were filtered at $<5\%$ FDR.

Cell culture and imaging

HeLa cells were cultured in DMEM with 4.5 g/l glucose, 5.84 g/l L-glutamine, 10% heat inactivated FBS, 100 IU/ml penicillin, and 100 μg/ml streptomycin as previously described (Wilson *et al*, 2005).

For time-lapse microscopy, FIP3–GFP-expressing HeLa cells were plated on collagen-coated cover slips. After 24 h incubation, cells were mounted on PH2-heated platform fitted with a TC-344B dual automatic temperature controller (Warner Instruments). Cells were imaged at 37°C on an inverted microscope (Zeiss Axiovert 200M) using a $\times 63$ oil immersion lens. Images were acquired and analysed using Intelligent Imaging Innovations 3D rendering and exploration software. Time-lapse images (exposure 500 ms) were taken every 500 ms. For each series, 50 images were taken. Only low-level expressing cells were used for time-lapse analysis. To quantitate the direction (to and from mid-body) of organelle movement in FIP3–GFP expressing cells, 92 organelles from five randomly chosen cells were used for analysis. Only organelles that could be followed in at least four consecutive time-lapse images were included in final analysis.

For FRAP and FLIP analysis, HeLa cells stably expressing FIP3–GFP were mounted on PH2-heated platform fitted with a TC-344B dual automatic temperature controller (Warner Instruments). Cells were imaged at 37°C on a Zeiss LSM 510 NLO laser scanning confocal microscope with META detector for capturing emission spectra (UCHSC Light Microscopy Facility at Anshutz campus). Selected areas (furrow or centrosome-associated FIP3–GFP) were photobleached by ~ 3 s pulse of high-level 488 nm laser light. The recovery of FIP3–GFP fluorescence (FRAP) in bleached area or loss of fluorescence (FLIP) in other selected areas of the cell was analysed every minute for 5 min using $\times 63$ objective with the pinhole set for an approximate 1 μm optical slice. Six to eight randomly chosen cells were used for analysis.

To quantitate the levels of FIP3–GFP, ECT2 and Cyk-4 at the mid-body, randomly chosen mitotic cells stably expressing FIP3–GFP were analysed. Cells were classified into four main groups: anaphase, early telophase, mid-telophase and late telophase (see Figure 7B). The small square was then drawn around the mid-body and the fluorescence intensity of FIP3–GFP, Cyk-4 and ECT2 was analysed. The data were expressed as ratios between ECT2/Cyk-4, FIP3–GFP/Cyk-4 and FIP3–GFP/ECT2.

RNA interference

FIP3, ECT2 and MKLP1siRNA duplexes were previously described and were shown to specifically knockdown corresponding proteins (Fielding *et al*, 2005; Wilson *et al*, 2005; Yuce *et al*, 2005) (Supplementary Figure 5). Aurora B siRNA was designed based on human cDNA (5′-aatcaattgtgaagtgccgcg-3′) (Supplementary Figure 5). To knockdown FIP3, Aurora B, ECT2, Cyk-4 or MKLP1 HeLa cells were transfected with 20 nM siRNA using Lipofectamine 2000 (Invitrogen) using manufacturer's protocol. Transfected cells were incubated for 72 h, plated on collagen-coated cover slips and imaged using fluorescence microscopy as described above.

Expression constructs and protein purification

Myc-tagged ECT2(1–333) was created by cloning it into pCMV-Tag3a (Stratagene, La Jolla, CA) vector using *Eco*RI and *Xho*I sites. Full-length FIP3–GFP was described previously (Wilson *et al*, 2005). HeLa Cells were transfected using a Gene Pulser Xcell (Bio-Rad, Hercules, CA) according to the manufacturer's protocol.

FIP3(441–756), FIP3(610–756), Rip11/FIP5, RCP/FIP1, Cyk-4, Cyk-4-Nt(1–234), Cyk-4-GAP(234–632), ECT2-N(1–333), ARF6, Rab11a, MKLP1(445–620) were expressed as a GST fusion proteins using pGEX-KG plasmid (Amersham Biosciences, Piscataway, NJ). GST fusion constructs were expressed using BL21-RIPL *Escherichia coli* strain. Proteins were purified using glutathione beads (Sigma-Aldrich, St Louis, MO) and either left on the beads or eluted by cleaving with thrombin (Amersham).

HeLa cell synchronization

HeLa cells were synchronized using thymidine/nocodazole block (Harper, 2005). Briefly, HeLa cells were incubated for 16 h in the presence of 5 mM thymidine. Cells were then washed and incubated in fresh serum-supplemented media. After 8 h, 100 ng/ml of nocodazole was added and cells were incubated for another 16 h. Cells arrested in metaphase were then dislodged by gently tapping to the side of the dish. Cells were collected and released from nocodazole mitotic block by washing in serum-supplemented media. After release from thymidine/nocodazole block, HeLa cells reach late telophase in approximately 3 h (Supplementary Figure 2).

Supplementary data

Supplementary data are available at *The EMBO Journal* Online (http://www.embojournal.org).

Acknowledgements

We thank Dr Toshio Kitamura (University of Tokyo) and Dr Andrew Peden (Cambridge University) for providing anti-Cyk-4/MgcRacGAP and anti-GFP antibodies. We also thank Dr Steven Fadul for all the help with FRAP and FLIP microscopy. This study was in part supported by grants from The Wellcome Trust (studentship to XY, Research Leave Award to GWG) and the NIH-NIDDK (grant DK064380 to RP).

References

Baluska F, Menzel D, Barlow PW (2006) Cytokinesis in plant and animal cells: endosomes 'shut the door'. *Dev Biol* **294:** 1–10

Boucrot E, Kirchhausen T (2007) Endosomal recycling controls plasma membrane area during mitosis. *Proc Natl Acad Sci USA* **104:** 7939–7944

Chalamalasetty RB, Hummer S, Nigg EA, Sillje HH (2006) Influence of human Ect2 depletion and overexpression on cleavage furrow formation and abscission. *J Cell Sci* **119:** 3008–3019

Chen XW, Inoue M, Hsu SC, Saltiel AR (2006) RalA-exocyst-dependent recycling endosome trafficking is required for the completion of cytokinesis. *J Biol Chem* **281:** 38609–38616

Eathiraj S, Mishra A, Prekeris R, Lambright DG (2006) Structural basis for Rab11-mediated recruitment of FIP3 to recycling endosomes. *J Mol Biol* **364:** 121–135

Fielding AB, Schonteich E, Matheson J, Wilson G, Yu X, Hickson GR, Srivastava S, Baldwin SA, Prekeris R, Gould GW (2005) Rab11-FIP3 and FIP4 interact with Arf6 and the exocyst to control membrane traffic in cytokinesis. *EMBO J* **24:** 3389–3399

Gromley A, Yeaman C, Rosa J, Redick S, Chen CT, Mirabelle S, Guha M, Sillibourne J, Doxsey SJ (2005) Centriolin anchoring of exocyst and SNARE complexes at the midbody is required for secretory-vesicle-mediated abscission. *Cell* **123:** 75–87

Guse A, Mishima M, Glotzer M (2005) Phosphorylation of Zen-4/MKLP1 by aurora b regulates completion of cytokinesis. *Curr Biol* **15:** 778–786

Hales CM, Griner R, Hobdy-Henderson KC, Dorn MC, Hardy D, Kumar R, Navarre J, Chan EK, Lapierre LA, Goldenring JR (2001) Identification and characterization of a family of Rab11-interacting proteins. *J Biol Chem* **276:** 39067–39075

Harper JV (2005) Synchronization of cell populations in G1/S and G2/M phases of the cell cycle. *Methods Mol Biol* **296:** 157–166

Hickson GRX, Matheson J, Riggs B, Maier VH, Fielding AB, Prekeris R, Sullivan W, Barr FA, Gould GW (2003) Arfophilins are dual Arf/Rab11 binding proteins that regulate recycling endosome distribution and are related to *Drosophila* nuclear fallout. *Mol Biol Cell* **14:** 2908–2920

Horgan CP, Walsh M, Zurawski TH, McCaffrey MW (2004) Rab11–FIP3 localises to a Rab11-positive pericentrosomal compartment during interphase and to the cleavage furrow during cytokinesis. *Biochem Biophys Res Commun* **319:** 83–94

Jagoe WN, Lindsay AJ, Read RJ, McCoy AJ, McCaffrey MW, Khan AR (2006) Crystal structure of rab11 in complex with rab11 family interacting protein 2. *Structure* **14:** 1273–1283

Janetopoulos C, Borleis J, Vazquez F, Iijima M, Devreotes P (2005) Temporal and spatial regulation of phosphoinositide signaling mediates cytokinesis. *Dev Cell* **8:** 467–477

Jantsch-Plunger V, Gonczy P, Romano A, Schnabel H, Hamill D, Schnabel R, Hyman AA, Glotzer M (2000) CYK-4: a Rho family gtpase activating protein (GAP) required for central spindle formation and cytokinesis. *J Cell Biol* **149:** 1391–1404

Kamijo K, Ohara N, Abe M, Uchimura T, Hosoya H, Lee JS, Miki T (2006) Dissecting the role of Rho-mediated signaling in contractile ring formation. *Mol Biol Cell* **17:** 43–55

Kitamura T, Kawashima T, Minoshima Y, Tonozuka Y, Hirose K, Nosaka T (2001) Role of MgcRacGAP/Cyk4 as a regulator of the small GTPase Rho family in cytokinesis and cell differentiation. *Cell Struct Funct* **26:** 645–651

Kouranti I, Sachse M, Arouche N, Goud B, Echard A (2006) Rab35 regulates an endocytic recycling pathway essential for the terminal steps of cytokinesis. *Curr Biol* **16:** 1719–1725

Low SH, Li X, Miura M, Kudo N, Quinones B, Weimbs T (2003) Syntaxin 2 and endobrevin are required for the terminal step of cytokinesis in mammalian cells. *Dev Cell* **4:** 753–759

Meyers JM, Prekeris R (2002) Formation of mutually exclusive Rab11 complexes with members of the family of Rab11-interacting proteins regulates Rab11 endocytic targeting and function. *J Biol Chem* **277:** 49003–49010

Mishima M, Kaitna S, Glotzer M (2002) Central spindle assembly and cytokinesis require a kinesin-like protein/RhoGAP complex with microtubule bundling activity. *Dev Cell* **2:** 41–54

Nishimura Y, Yonemura S (2006) Centralspindlin regulates ECT2 and RhoA accumulation at the equatorial cortex during cytokinesis. *J Cell Sci* **119:** 104–114

Peden AA, Schonteich E, Chun J, Junutula JR, Scheller RH, Prekeris R (2004) The RCP–Rab11 complex regulates endocytic protein sorting. *Mol Biol Cell* **15:** 3530–3541

Prekeris R (2003) Rabs, Rips, FIPs, endocytic membrane traffic. *Sci World J* **3:** 870–880

Prekeris R, Davies JM, Scheller RH (2001) Identification of a novel Rab11/25 binding domain present in Eferin and Rip proteins. *J Biol Chem* **276:** 38966–38970

Prekeris R, Gould GW (2008) Breaking up is hard to do: membrane traffic and cytokinesis. *J Cell Sci* **121:** 1569–1576

Prekeris R, Klumperman J, Scheller RH (2000) A Rab11/Rip11 protein complex regulates apical membrane trafficking via recycling endosomes. *Mol Cell* **6:** 1437–1448

Prigent M, Dubois T, Raposo G, Derrien V, Tenza D, Rosse C, Camonis J, Chavrier P (2003) ARF6 controls post-endocytic recycling through its downstream exocyst complex effector. *J Cell Biol* **163:** 1111–1121

Riggs B, Rothwell W, Mische S, Hickson GR, Matheson J, Hays TS, Gould GW, Sullivan W (2003) Actin cytoskeleton remodeling during early *Drosophila* furrow formation requires recycling endosomal components nuclear-fallout and Rab11. *J Cell Biol* **163:** 143–154

Rothwell WF, Fogarty P, Field CM, Sullivan W (1998) Nuclear-fallout, a *Drosophila* protein that cycles from the cytoplasm to the centrosomes, regulates cortical microfilament organization. *Development* **125:** 1295–1303

Saito S, Liu XF, Kamijo K, Raziuddin R, Tatsumoto T, Okamoto I, Chen X, Lee CC, Lorenzi MV, Ohara N, Miki T (2004) Deregulation and mislocalization of the cytokinesis regulator ECT2 activate the Rho signaling pathways leading to malignant transformation. *J Biol Chem* **279:** 7169–7179

Schonteich E, Pilli M, Simon GC, Matern HT, Junutula JR, Sentz D, Holmes RK, Prekeris R (2007) Molecular characterization of Rab11–FIP3 binding to Arf GTPases. *Eur J Cell Biol* **86:** 417–431

Schweitzer JK, Burke EE, Goodson HV, D'Souza-Schorey C (2005) Endocytosis resumes during late mitosis and is required for cytokinesis. *J Biol Chem* **280:** 41628–41635

Schweitzer JK, D'Souza-Schorey C (2002) Localization and activation of the ARF6 GTPase during cleavage furrow ingression and cytokinesis. *J Biol Chem* **277:** 27210–27216

Schweitzer JK, D'Souza-Schorey C (2005) A requirement for ARF6 during the completion of cytokinesis. *Exp Cell Res* **311:** 74–83

Shiba T, Koga H, Shin HW, Kawasaki M, Kato R, Nakayama K, Wakatsuki S (2006) Structural basis for Rab11-dependent membrane recruitment of a family of Rab11-interacting protein 3 (FIP3)/Arfophilin-1. *Proc Natl Acad Sci USA* **103:** 15416–15421

Shin OH, Couvillon AD, Exton JH (2001) Arfophilin is a common target of both class II and class III ADP-ribosylation factors. *Biochemistry* **40:** 10846–10852

Shin OH, Ross AH, Mihai I, Exton JH (1999) Identification of arfophilin, a target protein for GTP-bound class II ADP-ribosylation factors. *J Biol Chem* **274:** 36609–36615

Shuster CB, Burgess DR (2002) Targeted new membrane addition in the cleavage furrow is a late, separate event in cytokinesis. *Proc Natl Acad Sci USA* **99:** 3633–3638

Skop AR, Bergmann D, Mohler WA, White JG (2001) Completion of cytokinesis in *C. elegans* requires a brefeldin A-sensitive membrane accumulation at the cleavage furrow apex. *Curr Biol* **11:** 735–746

Toure A, Dorseuil O, Morin L, Timmons P, Jegou B, Reibel L, Gacon G (1998) MgcRacGAP, a new human GTPase-activating protein for Rac and Cdc42 similar to *Drosophila* rotundRacGAP gene product, is expressed in male germ cells. *J Biol Chem* **273:** 6019–6023

Wilson GM, Fielding AB, Simon GC, Yu X, Andrews PD, Hames RS, Frey AM, Peden AA, Gould GW, Prekeris R (2005) The FIP3–Rab11 protein complex regulates recycling endosome targeting to the cleavage furrow during late cytokinesis. *Mol Biol Cell* **16:** 849–860

Yu X, Prekeris R, Gould GW (2007) Role of endosomal Rab GTPases in cytokinesis. *Eur J Cell Biol* **86:** 25–35

Yuce O, Piekny A, Glotzer M (2005) An ECT2-centralspindlin complex regulates the localization and function of RhoA. *J Cell Biol* **170:** 571–582

Zhang XM, Ellis S, Sriratana A, Mitchell CA, Rowe T (2004) Sec15 is an effector for the Rab11 GTPase in mammalian cells. *J Biol Chem* **279:** 43027–43034

Zhao WM, Fang G (2005) MgcRacGAP controls the assembly of the contractile ring and the initiation of cytokinesis. *Proc Natl Acad Sci USA* **102:** 13158–13163